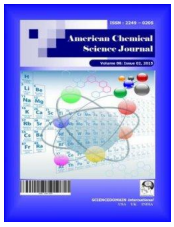

American Chemical Science Journal
8(2): 1-16, 2015, Article no.ACSj.18211
ISSN: 2249-0205

SCIENCEDOMAIN *international*
www.sciencedomain.org

Corrosion Inhibition Behaviour and Adsorption Characteristics of Dapsone Derivatives on Mild Steel in Acid Medium

M. P. Chakravarthy[1], K. N. Mohana[1*], C. B. Pradeep Kumar[2] and A. M. Badiea[3]

[1]Department of Studies in Chemistry, University of Mysore, Manasagangothri, Mysore, 570 006, India.
[2]Department of Chemistry, Sarada Vilas College, Mysore-570 005, India.
[3]Department of Industrial and Manufacturing System Engineering, Engineering College and IT, Taiz University, Yemen.

Authors' contributions

This work was carried out in collaboration between all authors. Author MPC designed the study, performed the statistical analysis, wrote the protocol, and wrote the first draft of the manuscript. Authors KNM and CBPK managed the analyses of the study. Author AMB managed the literature searches. All authors read and approved the final manuscript.

Article Information

DOI: 10.9734/ACSj/2015/18211
Editor(s):
(1) Ling Bing Kong, School of Materials Science and Engineering, Nanyang Technological University, Singapore.
Reviewers:
(1) Ugi, Benedict Ushaka, Pure and Applied Chemistry, University of Calabar, Nigeria.
(2) Anonymous, V. R. Siddhartha Engineering College, India.
(3) Anonymous, Madras University, Tamilnadu, India.
Complete Peer review History: http://www.sciencedomain.org/review-history.php?iid=1161&id=16&aid=9733

Original Research Article

Received 9th April 2015
Accepted 27th May 2015
Published 12th June 2015

ABSTRACT

Two newly synthesized Dapsone derivatives viz., 3-[(4-{4-[(1H-Indol-3-ylmethylene)-amino]-benzenesulfonyl}-phenylimino)-methyl]-1H-indole (IABPI) and 5-[(4-{4-[(Thiophen-2-ylmethylene)-amino]-benzenesulfonyl}-phenylimino)-methyl]-thiophene (TABPT) were investigated as corrosion inhibitors for mild steel in 0.5 M H_2SO_4 media by using chemical and electrochemical techniques. Potentiodynamic polarization studies indicated that these two inhibitors behaved as mixed type. These inhibitors were found to obey Langmuir isotherm model. Using this isotherm, thermodynamic adsorption parameters were evaluated. EIS studies showed that the polarization resistance (R_P) and double layer capacitance (C_{dl}) of the inhibitors are concentration dependent. FTIR technique was used to identify the interaction of inhibitor with mild steel surface, whereas persistency of thin protective film of inhibitors on the mild steel surface was carried out by using EDX and SEM.

**Corresponding author: E-mail: drknmohana@gmail.com*

Keywords: Mild steel; dapsone derivatives; chemical and electrochemical techniques; SEM.

1. INTRODUCTION

Metals and alloys are susceptible to different corrosion mechanisms, when they are exposed to different corrosive media, especially in acidic media, which is largely used in industries [1]. Among these, mild steel (MS) is extensively used, which is an alloy of iron, carbon and several other elements. Inhibitors are widely used for protection of metals from corrosion in acid environments. Generally, the selection of an appropriate inhibitor depends on its capacity to inhibit corrosion of metallic materials, its environmental side effects and its economic viability.

The study of MS corrosion in different acid media is common due to the use of acid solutions in industries [2-7]. Among the acid solutions, sulfuric acid is one of the most aggressive acids for iron and its alloys and is often used during cleaning, pickling, descaling and other purposes. Addition of corrosion inhibitors is one of the methods to minimize the rate of metallic corrosion. Most of the well known acid inhibitors are organic compounds containing nitrogen, oxygen and sulfur atoms which determine the mode of interaction of inhibitor on the MS surface.

These inhibitors reduce the active sites their by decreases the rate of metal dissolution and enhances the quality as well as life span of the metallic materials [8,9]. Many reports showed that organic molecules may undergo physisorption or chemisorption or both on the metallic surfaces their by retarding the corrosion rate. In general, organic compounds containing O, N, S atoms and multiple bonds show better inhibition efficiency than organic molecules containing N or S alone [10,11].

Molecules containing more number of heteroatoms are of interest because of their strong chemical activity, low toxicity and environmental friendly characteristics as corrosion inhibitors [12]. The physical and chemical adsorption processes of organic molecules depend on the nature and surface charge of the metal, nature of interaction and structure of corrosion inhibitors and the type of aggressive media [13-17]. Usually, sulphur containing compounds are more effective corrosion inhibitors than the corresponding nitrogen compounds since sulphur is better electron donor than nitrogen and easily adsorb on metallic surfaces. Sulphonium and sulphoxides are recommended as inhibitors in acids mainly in sulphuric acid solution.

Several nitrogen, oxygen and sulphur containing heterocyclic compounds such as phenylhydrazone derivatives [18], acetyl pyridine derivatives [19], diphenyl-vinyl-imidazole derivatives [20], pyrimidine derivatives [21], formazan derivatives [22], quinoxaline derivatives [23], salts of lauric hydrazide [24], pyridine derivatives [25], triazoles [26] and fluoroquinolone molecules [27] are reported as corrosion inhibitors.

The present work is mainly focused on the investigation of corrosion inhibition action of two newly synthesized dapsone derivatives, i.e., 3-[(4-{4-[(1H-Indol-3-ylmethylene)-amino]-benzenesulfonyl}-phenylimino)-methyl]-1H-indole (IABPI) and 5-[(4-{4-[(Thiophen-2-ylmethylene)-amino]-benzenesulfonyl}-phenylimino)-methyl]-thiophene (TABPT) in 0.5 M H_2SO_4 on mild steel (MS) by non-electrochemical (mass loss) and electrochemical methods. The experimental results were discussed. The protective film formed on the surface of MS was characterized by EDX and SEM. The interaction of inhibitor on the MS surface was studied by FTIR technique.

2. EXPERIMENTAL DETAILS

2.1 Mild Steel Specimen Preparation

Mild steel specimens of 2 cm × 2 cm × 0.1 cm dimensions were employed for the determination of mass loss measurements. The chemical composition of MS specimens used in the experimental studies having the chemical compositions (in wt %) of C 0.051; Pb 0.001; Nb 0.012; Al 0.103; Ni 0.05; Sn 0.004; Cu 0.050; P 0.005; S 0.023; Cr 0.051; Ti 0.004; Mo 0.013; B 0.00105; Co 0.017; Si 0.006; Mn 0.179 and the remaining left out portion is iron. All the experimental studies were carried out using thoroughly well mechanically polished MS specimens with silicon carbide (200 - 600 grades) emery papers. Degreased with benzene and washed with triple distilled water and finally air dried after rinsing with acetone. The chemicals and solvents used are of AR grade, used as it is. Triple distilled water is used for the preparation of test solutions of various concentrations.

2.2 Synthesis of Inhibitors

IABPI was synthesized by dissolving 2.5 mmol (0.62 g) of dapsone (Mol. Wt. 248.30, $C_{12}H_{12}N_2O_2S$) in methanol (15 mL) taken in thoroughly cleaned round bottom flask. For this 5 mmol (0.72 g) of indole-3-carboxaldehyde (Mol. Wt. 145.16, C_9H_7NO) in methanol (15 mL) was added and at 60ºC temperature it was refluxed nearly for 6 hr in presence of few drops of glacial acetic acid. The solution obtained was concentrated by rotor vaporizer and vacuum dried. Similarly, TABPT was synthesized by dissolving 2.5 mmol (0.62 g) of dapsone in methanol (15 mL) in a well cleaned round bottom flask. To this 5 mmol (0.5 mL) of 2-thiophenecarboxaldehyde (Mol. Wt. 112.15, C_5H_4OS) in methanol (15 mL) was added and at 60°C temperature it was refluxed nearly for 6 hr in presence of few drops of glacial acetic acid, and the obtained solution was concentrated by rotor vaporizer and vacuum dried. The scheme of synthesis of IABPI and TABPT are shown in Fig. 1.

The characterization and structural confirmation of compounds are established by Mass, ^{1}H-NMR and FTIR spectral studies. IABPI ($C_{30}H_{22}N_4O_2S$): Mol. Wt. 502.59, Melting Range (°C): 150 – 152, % Yield: 87. Elemental analyses found (calculated) for IABPI (%): C, 71.66 (71.69): H, 4.38 (4.41): N, 11.09 (11.15), O, 6.34 (6.37), S, 6.33 (6.38). Maas Spectra, m/z: 503 (M+1 peak), ^{1}H-NMR δ ppm (DMSO-d6, 400.15 MHz): 9.2 (s, 2H), 8.34 (s, 2H), 8.21-8.19 (m, 2H), 7.81-7.79 (d, J = 8.0 Hz, 2H), 7.72-7.70 (d, J = 8.2 Hz, 2H), 7.57 (s, 2H), 7.54-7.52 (m, 2H), 7.51-7.49 (d, J = 7.8 Hz, 2H), 7.47-7.45 (d, J = 8.0 Hz, 2H), 7.21-7.19 (m, 2H), 7.11-7.08 (m, 2H). FTIR (KBr Pellets, cm^{-1}): 1145 (symmetric-SO_2-streching), 1277 (asymmetric-SO_2-streching), 1589 (N=C), 1633 (C=N).

TABPT ($C_{22}H_{16}N_2O_2S_3$): Mol. Wt. 436.57, Melting Range (°C): 168 – 170, Yield: 82%. Elemental analyses found (calculated) for TABPT (%): C, 60.51 (60.53): H, 3.66 (3.69): N, 6.39 (6.42), O, 7.31 (7.33), S, 21.98 (22.03). MS, m/z: 437 (M+1 peak). ^{1}H-NMR δ ppm (DMSO-d6, 400.15 MHz): 7.16-7.13 (t, 2H), 7.42-7.743 (d, J = 7.8 Hz, 2H), 7.51-7.49 (d, J = 8.2 Hz, 2H), 7.64-7.62 (d, J = 8.8 Hz, 2H), 7.69-7.67 (d, J = 8.2 Hz, 2H), 7.72-7.70 (d, J = 7.6 Hz, 2H), 7.79-7.80 (d, J = 8.5 Hz, 2H), 8.36 (s, 2H). FTIR (KBr Pellets, cm^{-1}): 1138 (symmetric-SO_2-streching), 1299 (asymmetric-SO_2-streching), 1592 (N=C), 1613 (C=N). The melting range was found using Veego Melting Point III apparatus. Elemental analyses of inhibitors were determined using Vario MICRO superuser V1.3.2 elementar apparatus. LC/MSD Trap XCT apparatus was employed for taking mass spectral data of inhibitors. Using Bruker DRX-500 spectrometer ^{1}H-NMR spectra were recorded at 400 MHz using TMS as an internal standard and DMSO-d_6 as solvent. Jasco FTIR 4100 double beam spectrophotometer was used to record the FTIR spectra of inhibitor molecules.

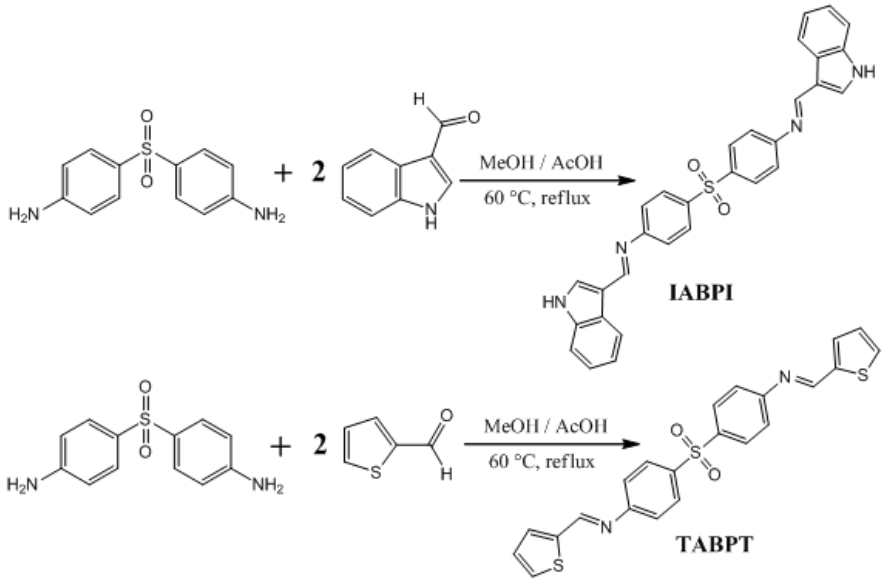

Fig. 1. Synthetic scheme of IABPI and TABPT

2.3 Mass Loss Measurements

The Mass loss measurements were monitored at 303, 313, 323 and 333 K by weighing well cleaned and completely dried MS specimens for a period of one to five hours, before and after immersion in 0.5 M H_2SO_4 solutions in the absence and presence of 200, 300, 400 and 500 ppm concentrations of IABPI and TABPT. For the accuracy of the result, the experiments were performed in triplicate and the mean value was recorded. Calculations of corrosion rate and inhibition efficiency IE_{ML} (%) were done using the relations (1) and (2).

$$CR = \frac{\Delta M}{St}, \quad (1)$$

where t : time of immersion, S : surface area of the MS specimen and ΔM : Mass loss value.

$$IE_{ML}\ (\%) = \frac{(CR)_a - (CR)_p}{(CR)_a} \times 100, \quad (2)$$

where $(CR)_a$ and $(CR)_p$ are the corrosion rate values with and without the inhibitor.

2.4 Potentiodynamic Polarization Curves

The electrochemical behavior of MS specimens in the absence and presence of inhibitors was studied by recording anodic and cathodic polarization curves. Measurements were performed in 0.5 M H_2SO_4 solution with MS as working electrode containing different concentrations of the inhibitor with an exposed area of 1 cm^2 in the experiment. A three electrode conventional cell with MS working electrode, platinum foil as counter electrode and *saturated calomel* reference electrode were used. CH-instrument model CHI660D was employed for the study of potentiodynamic polarization. Each polarization curve was taken by recording open circuit potential by allowing MS electrode to corrode up to 30 min with respect to the corrosion potential (E_{corr}). The IE_P (%) was calculated using the relation (3).

$$IE_P\ (\%) = \frac{(I_{corr})_a - (I_{corr})_p}{(I_{corr})_a} \times 100 \quad (3)$$

where $(I_{corr})_a$ and $(I_{corr})_p$ are the corrosion current densities without and with inhibitor.

2.5 Electrochemical Impedance Spectroscopy Measurement

Using CH-instrument model CHI660D in the frequency range 10 kHz to 100 mHz the electrochemical impedance spectroscopy parameters such as double layer capacitance (C_{dl}) and the polarization resistance (R_p) were determined through Nyquist plots [28]. Further, taking R_p values, IE_{EIS} (%) was calculated using the following expression:

$$IE_{EIS}(\%) = \frac{{}^{1}/_{(R_p)_a} - {}^{1}/_{(R_p)_p}}{{}^{1}/_{(R_p)_a}} \times 100 \quad (4)$$

where $(R_p)_a$ and $(R_p)_p$ are polarization resistances without and with the inhibitor.

2.6 FTIR, EDX and SEM Studies

The interaction of inhibitors with MS surface was determined using FTIR spectral studies. MS specimens immersed in the presence of inhibitor of 500 ppm in 0.5 M H_2SO_4 for a period of 1 h was taken out, dried and the surface adheared thin film was carefully scratched and its FTIR spectra was recorded. The surface morphology of the MS specimens in the absence and presence of inhibitors was studied by using energy dispersive X-ray spectroscopy (EDX) and scanning electron microscopy (SEM) studies.

3. RESULTS AND DISCUSSION

3.1 Mass Loss Studies

Table 1 shows mass loss parameters such as corrosion rate (CR) and percentage inhibition efficiency IE_{ML} (%) in 0.5 M H_2SO_4 at 303, 313, 323 and 333 K in the absence and presence of 200, 300, 400 and 500 ppm concentrations of IABPI and TABPT. The observations showed that decrease in mass loss and increases in IE_{ML} (%) are concentration dependent. The maximum inhibition efficiency was attained at 500 ppm, beyond this concentration there is no any remarkable change in the inhibition efficiency for 1h of immersion period. It is due to desorption of inhibitor from MS surface and instability of inhibitor coating on the MS surface [29,30].

3.2 Variation of Temperature

The corrosion rate (CR) and IE_{ML} (%) have been evaluated in the absence and presence of 200,

300, 400 and 500 ppm concentrations of inhibitors in 0.5 M H_2SO_4 at various temperature. Studies showed that with the raise in temperature from 303 – 333 K, there was a gradual decrease and increase in percentage of inhibition efficiency and corrosion rate, respectively due to desorption of inhibitor from MS surface and the data are tabulated in Table 1. From the following Arrhenius equation, the activation parameters were computed.

$$CR = k\ exp^{-Ea/RT} \quad (5)$$

where T : Absolute temperature, R : Universal gas constant, k : frequency factor, and E_a : activation energy. The activation energy for MS corrosion in the absence and presence of 200 – 500 ppm concentrations of inhibitors were obtained from the slope of plot log CR versus 1/T (Fig. 2) and are presented in Table 2.

Table 1. CR and IE_{ML} (%) in 0.5 M H_2SO_4 solution containing 0, 200, 300, 400 and 500 ppm concentrations of IABPI and TABPT at 303, 313, 323 and 333 K

T (K)	C (ppm)	IABPI		TABPT	
		CR (mg cm^{-2} h^{-1})	IE_{ML} (%)	CR (mg cm^{-2} h^{-1})	IE_{ML} (%)
303	0	1.0260	-	1.0260	-
	200	0.1492	85.45	0.0979	90.45
	300	0.1376	86.58	0.0879	91.43
	400	0.1179	88.49	0.0680	93.36
	500	0.0956	90.67	0.0442	95.68
313	0	1.4170	-	1.4170	-
	200	0.2377	83.22	0.1685	88.10
	300	0.2166	84.71	0.1475	89.58
	400	0.1915	86.48	0.1218	91.40
	500	0.1667	88.22	0.0959	93.23
323	0	2.0400	-	2.0400	-
	200	0.3822	81.26	0.2815	86.19
	300	0.3520	82.74	0.2504	87.72
	400	0.3109	84.75	0.2114	89.63
	500	0.2605	87.22	0.1601	92.15
333	0	2.733	-	2.733	-
	200	0.6177	77.39	0.4833	82.31
	300	0.5729	79.03	0.4387	83.94
	400	0.5051	81.51	0.3676	86.54
	500	0.4282	84.33	0.2925	89.29

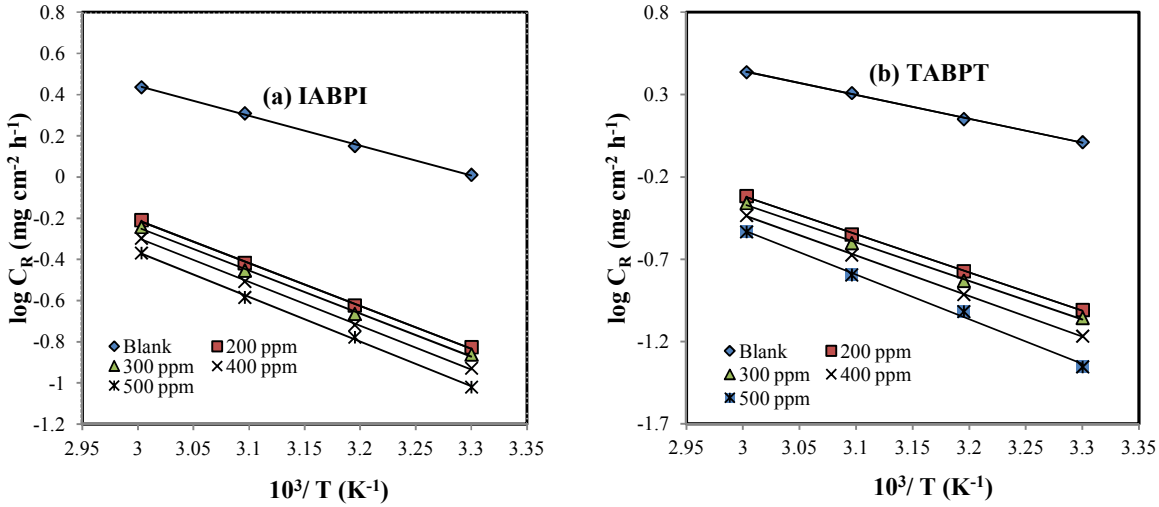

Fig. 2. Plot of log CR versus 1/T for IABPI and TABPT

Table 2. Activation parameters for MS containing 0, 200, 300, 400 and 500 ppm concentrations of IABPI and TABPT in 0.5 M H_2SO_4

Inhibitor	C (ppm)	E_a (kJ mol^{-1})	ΔH_a (kJ mol^{-1})	$\Delta H_a = E_a - RT$ (kJ mol^{-1})	ΔS_a (J mol^{-1}K^{-1})
Blank	0	27.70	25.06	25.18	-197.57
IABPI	200	39.69	37.06	37.17	-138.71
	300	39.92	37.27	37.40	-138.69
	400	40.63	37.98	38.11	-137.56
	500	41.47	38.83	38.95	-136.34
TABPT	200	44.44	41.81	41.92	-126.50
	300	44.84	42.20	42.32	-126.19
	400	47.06	44.42	44.54	-120.85
	500	51.86	49.24	49.35	-108.15

It was found that experimental E_a in the presence of inhibitors are greater than those without inhibitors (Table 2). This higher value of activation energy retards the corrosion rate of MS [31]. Addition of inhibitor induces energy barrier and increases the activation energy for corrosion reaction and this barrier become greater with gradual raise in inhibitors concentration. As the temperature is increased, there is a considerable rise in corrosion rate due to desorption of the inhibitors from the MS surface. Using the relation (6), the activation thermodynamic parameters such as ΔH_a and ΔS_a were calculated from the plot of log CR/T versus 1/T (Fig. 3).

$$CR = \frac{RT}{Nh}\exp\left(\frac{\Delta S_a}{R}\right)\exp\left(\frac{-\Delta H_a}{RT}\right) \quad (6)$$

where *h*: Planks constant, *T*: absolute temperature, *N*: Avogadro's number and *R* : Universal gas constant.

The slope and intercept of the plot log CR/T versus 1/T gives the values of activation enthalpy, ΔH_a and activation entropy, ΔS_a (Table 2). The experimental data are in close agreement with calculated values through the equation (7),

$$\Delta H_a = E_a - RT \quad (7)$$

The values of ΔH_a, indicate the endothermic nature and also strong ability of adsorption of inhibitors on MS surface [32], whereas large negative values of ΔS shows minimum disorderness due to associative interaction of inhibitors on MS surface [33-35].

3.3 Mode of Adsorption

The adsorption isotherm study gives knowledge about the interaction of inhibitors on the metal surface. In general, the mode of adsorption of inhibitor may be physisorption or chemisorption or both. The inhibition efficiency of inhibitor mainly depends on the mode of adsorption on the metal surface. Quasi-substitution process is involved by the adsorbed inhibitor molecules which is *p*H dependent in aqueous solution [36]. Polarization and ionization factors of inhibitors also reveals mode of adsorption on MS [37]. By fitting degree of surface coverage (θ) and inhibitor concentration, the best adsorption isotherm obtained graphically, was Langmuir isotherm model in 0.5 M H_2SO_4 on MS and this adsorption isotherm was employed for determining adsorption thermodynamic parameters. Further, adsorption equilibrium constant (K_{ads}) and θ are related to the concentration of the inhibitor (C) through the expression (8):

$$C/\theta = \frac{1}{K_{ads}} + C \quad (8)$$

In all the cases, plot of C/θ versus C (Fig. 4) gave straight line with R^2 (linear regression coefficient) and slope values nearer to unity indicating that each inhibitor molecule occupies one active site on MS surface. Using the relation (9) free energy of adsorption was calculated as follows:

$$\Delta G^{\circ}_{ads} = -2.303RTlog55.5K_{ads} \quad (9)$$

where K_{ads}: adsoption equilibrium constant, *R*: Universal gas constant, *T*: absolute temperature, and 55.5: molar concentration of water in solution (mol L^{-1}).

From the slope and intercept obtained by the plot of log K_{ads} versus 1/T (Fig. 5), the thermodynamic adsorption parameters such as enthalpy of adsorption (ΔH^0_{ads}) and entropy of

adsorption (ΔS°_{ads}) were calculated using the relation (10).

$$\log K_{ads} = \frac{1}{2.303}\left(-\frac{\Delta H^{\circ}_{ads}}{RT}\right) + \left(\frac{\Delta S^{\circ}_{ads}}{R}\right) \quad (10)$$

The calculated values of K_{ads}, ΔH°_{ads}, ΔG°_{ads} and ΔS°_{ads} are recorded in Table 3 in the temperature range 303 – 333 K. The negative values of free energy of adsorption indicate the irreversible spontaneous adsorption of inhibitor on the MS [38]. In these studies, ΔG°_{ads} values of IABPI and TABPT are found to be in the range, -36.81 to -39.16 and -37.02 to -39.45 kJ mol^{-1}, respectively. The mode of adsorption mechanism involved is a comprehensive type i.e., involving both physisorption as well as chemisorption [39–42].

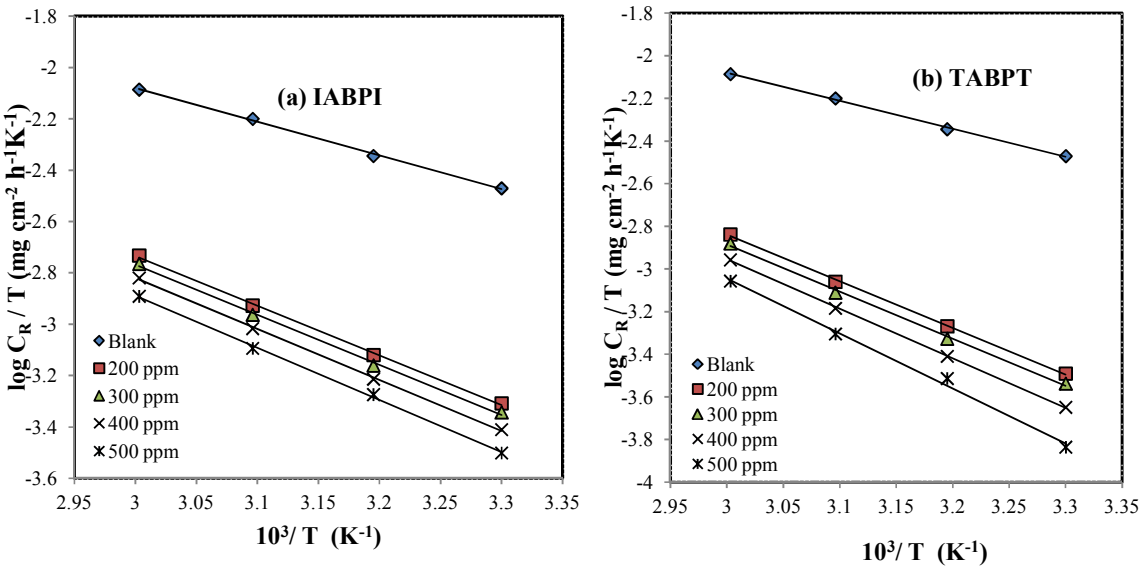

Fig. 3. Alternative Arrhenius plots for MS dissolution in the absence and presence of (a) IABPI and (b) TABPT in 0.5 M H_2SO_4

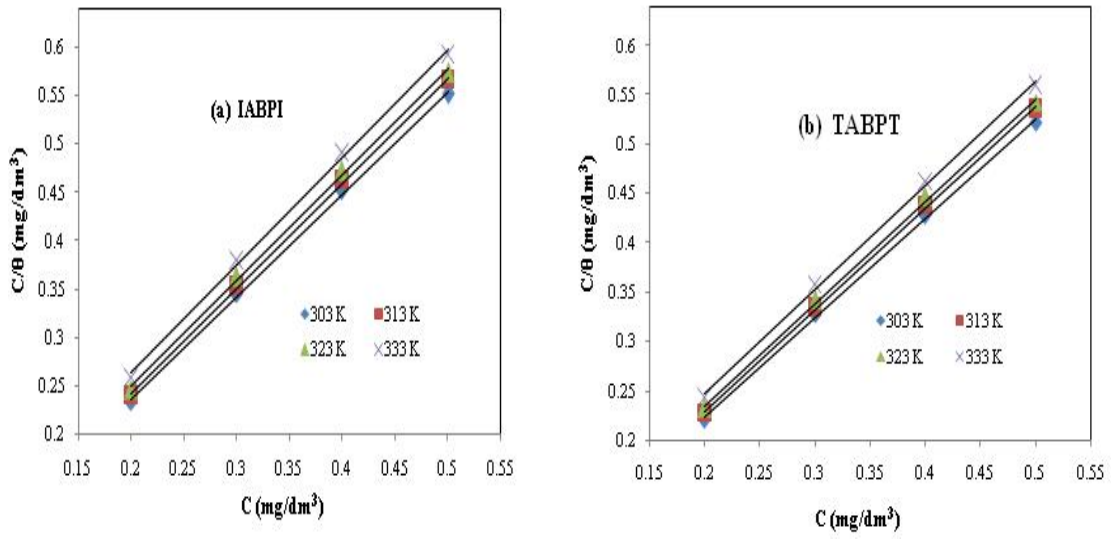

Fig. 4. Langmuir adsorption isotherm plots for IABPI and TABPT in 0.5 M H_2SO_4 on MS surface at 303, 313, 323 and 333 K

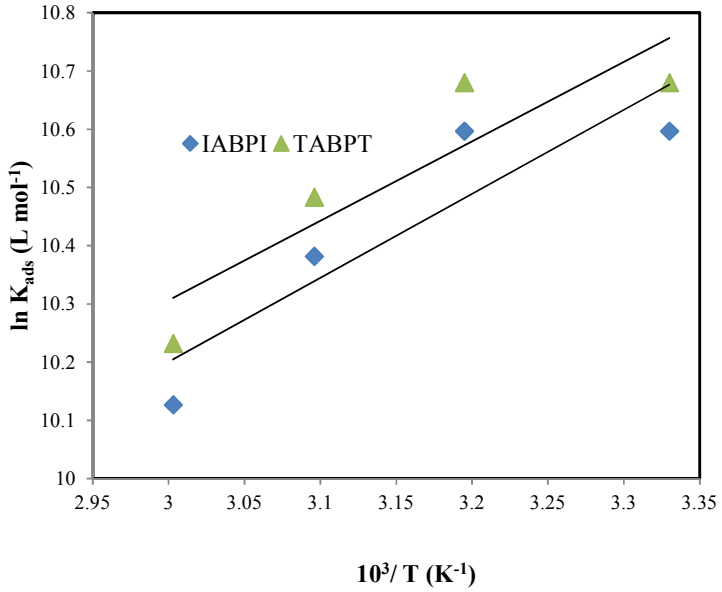

Fig. 5. Plots of lnK_{ads} versus 1/T for IABPI and TABPT

Table 3. Adsorption thermodynamic parameters of IABPI and TABPT on MS in 0.5 M H_2SO_4 at various temperature

Inhibitor	T (K)	R^2	Slope	$\Delta G°_{ads}$ (kJ mol^{-1})	$\Delta H°_{ads}$ (kJ mol^{-1})	$\Delta S°_{ads}$ (J mol^{-1} K^{-1})
IABPI	303	0.999	1.057	-36.81		
	313	0.999	1.087	-38.03	1.442	5.874
	323	0.999	1.09	-38.67		
	333	0.998	1.114	-39.16		
TABPT	303	0.999	1.004	-37.02		
	313	0.999	1.03	-38.25	1.366	6.207
	323	0.999	1.035	-38.94		
	333	0.998	1.055	-39.45		

3.4 FTIR Spectral Analysis

FTIR spectra were used to determine the active functional sites of inhibitors. FTIR spectra of pure IABPI and TABPT are shown in Figs. 6a and 7a, respectively. Figs. 6b and 7b are the scratched sample of MS surface adsorbed inhibitors.

Comparison of FTIR spectra of pure inhibitors and scratched inhibitor film adsorbed samples indicate that some of the active sites of inhibitors are involved in complex formation with MS surface and thereby reducing corrosion rate. In pure IABPI and TABPT peaks at 1589, 1633 and 1592, 1613 cm^{-1} are attributed to the azomethine group. But in the FTIR spectra of scratched samples, the azomethine group stretching frequencies are observed to be disappeared due to the involvement of azomethine groups in the formation of passive film complex.

3.5 Potentiodynamic Polarization Curves

Potentiodynamic polarization curves show the kinetics mechanism of both anodic and cathodic branches. Polarization curves for MS in 0.5 M H_2SO_4 in the absence and presence of 200 – 500 ppm of IABPI and TABPT at 30°C are shown in Fig. 8. Addition of IABPI and TABPT causes decrease in the rate of corrosion by shifting both anodic and cathodic curves to minimum values of corrosion current densities. Hence they are mixed type of inhibitors [43,44].

The polarization parameters such as corrosion current density (i_{corr}), corrosion potential (E_{corr}), cathodic Tafel slope (β_c), anodic Tafel slope (β_a) and percentage inhibition efficiency are presented in Table 4. The data revealed that the decrease in corrosion current density accompanying minimum corrosion rate resulting

in a very good corrosion protection due to the passive film formation on the surface of MS. It was also made clear that there was a gradual decrease of corrosion potential when the inhibitor concentration was changed from 200 ppm to 500 ppm.

The increase in IE_P (%) is due to the protective action of IABPI and TABPT via electron donating azomethine (–C=N–) group. The density of electron varies with the substituents present in the inhibitor molecules. The inhibition efficiency of TABPT is greater than that of IABPI, which is probably due to the difference in functional groups and hetero atoms in the structures of the inhibitors.

3.6 Electrochemical Impedance Spectroscopy

The Nyquist plots for MS in 0.5 M H_2SO_4 in the absence and presence of 200 – 500 ppm of IABPI and TABPT at 303 K are shown in Fig. 9. These plots exhibit a part of depressed semicircle which relates to heterogeneities, roughness, grain boundaries and distribution of the surface active sites like physical features [45].

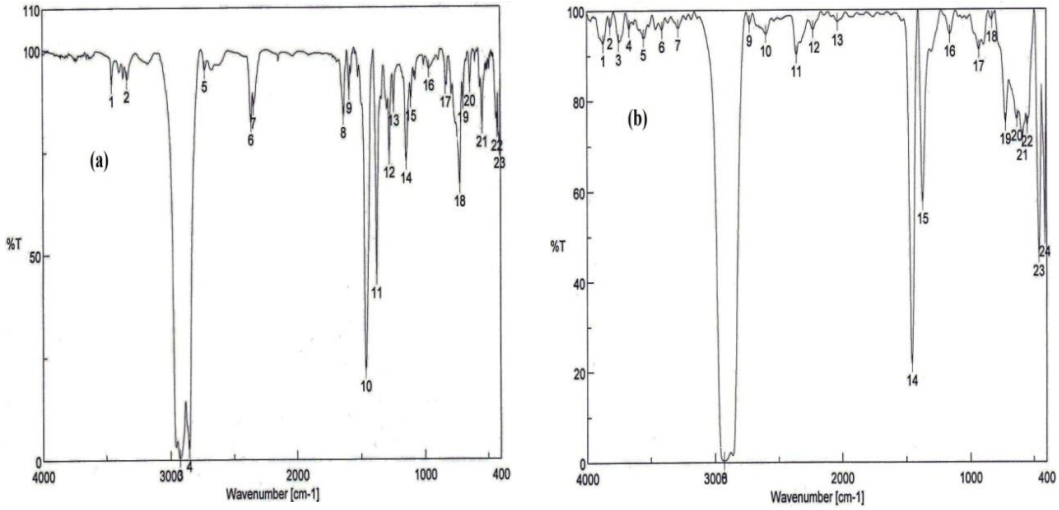

Fig. 6. FTIR spectra of (a) pure IABPI (b) scratched IABPI film adsorbed MS surface

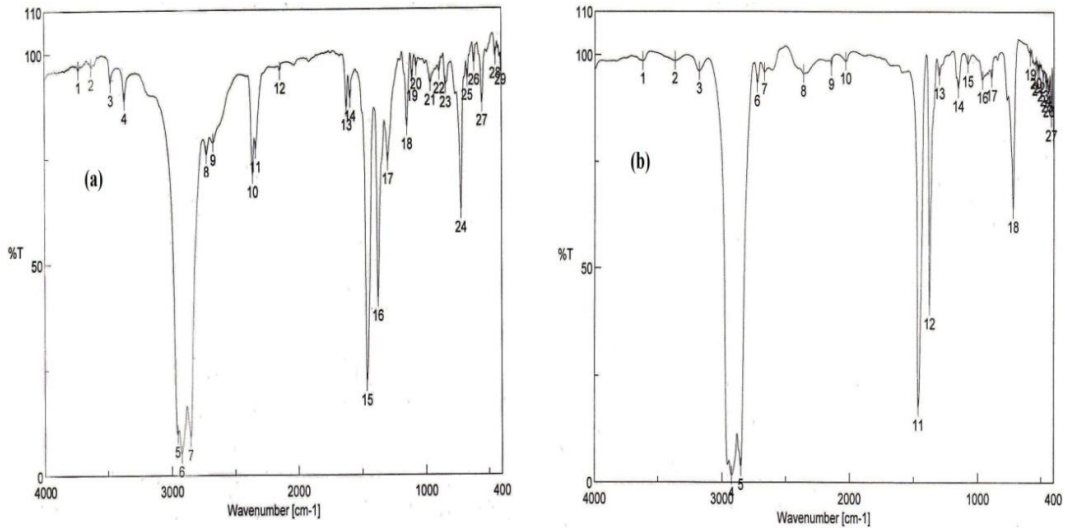

Fig. 7. FTIR spectra of (a) pure TABPT (b) scratched TABPT film adsorbed MS surface

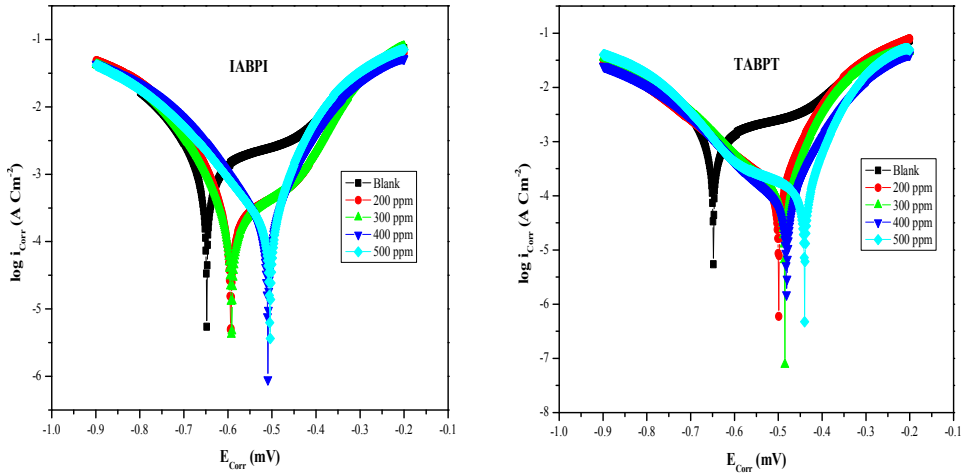

Fig. 8. Potentiodynamic polarization curves of MS without and with different concentrations of IABPI and TABPT in 0.5 M H_2SO_4

Table 4. Potentiodynamic polarization parameters without and with IABPI and TABPT on the corrosion of MS in 0.5 M H_2SO_4 at 303 K

Inhibitor	C (ppm)	$-\beta_c$ (mA dB^{-1})	β_a (mA dB^{-1})	$-E_{corr}$ (mV)	i_{corr} (μA Cm^{-2})	IE_P (%)
BLANK	0	8.088	2.212	0.648	1661	--
IABPI	200	14.104	3.638	0.595	260.2	84.34
	300	12.946	4.231	0.592	224.0	86.51
	400	7.977	11.562	0.509	193.8	88.33
	500	8.357	18.119	0.504	164.9	90.07
TABPT	200	6.119	16.207	0.499	157.5	90.51
	300	7.252	20.765	0.489	134.0	91.93
	400	7.205	16.841	0.485	103.2	93.78
	500	3.051	17.942	0.440	67.58	95.93

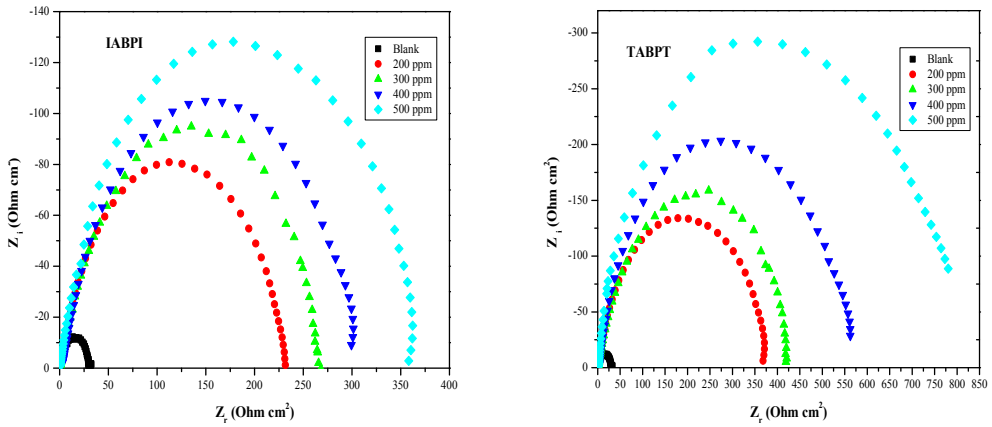

Fig. 9. Nyquist plots for MS corrosion in the absence and presence of IABPI and TABPT at 303 K

All the polarization parameters such as polarization resistance (R_p), double layer capacitance (C_{dl}) and percentage inhibition efficiency are presented in Table 5. The

interpretation of results showed that the corrosion rate was decreases gradually with the addition of inhibitors.

All the impedance data are obtained by equivalent circuit shown in the Fig. 10, in which double layer capacitance (C_{dl}) is parallel to polarization resistance (R_p) and are in series with solution resistance (R_s).

The experimental results showed that, as the inhibitors concentration is raised from 200-500 ppm there was a progressive increase in the diameter of each depressed semi-circle reflecting gradual increase in R_p values and gradual decrease in C_{dl} values. This is due to the reduction of MS corrosion rate [46,47] and also passive thin film formation at metal-solution interface. R_p values in the blank are always lower than that in the presence of inhibitors. The decrease in the double layer capacitance (C_{dl}) values is due to the decrease in local dielectric constant resulting in the formation of adsorbed inhibitor molecules at metal-solution interface [48,49] and also imperfection of the metal surface, results in the decrease of C_{dl} values [50,51]. Further, when immersion time is increased, a sudden increase and decrease in C_{dl} values and R_p values, respectively were observe reflecting desorption or instability of the protective film of the inhibitors.

3.7 Inhibition Mechanism

Corrosion inhibition of MS in 0.5 M H_2SO_4 solution by IABPI and TABPT can be made clear on the basis of molecular adsorption. The important type of interaction was found to be comprehensive mode of adsorption, i.e., involving both physical as well as chemical adsorption. The molecular adsorption mainly depends on the chemical structure of the inhibitor, morphology and nature of metal, electrolyte type and exposed temperature [52, 53]. The mode of adsorption between inhibitor and MS was donor-acceptor type. Adsorption of inhibitors is mainly due to the lone pair of electrons, number of heteroatoms and π-electrons of multiple bonds [54]. The inhibition mechanism of both IABPI and TABPT is due the presence of multiple π-electrons, hetero atoms and azomethine groups in the structures of the molecules. The inhibition efficiency of TABPT is higher than that of IABPI which is due to the presence of electron donating sulphur atom in the thiophene ring system.

Table 5. Impedance parameters for MS corrosion without and with 200-500 ppm IABPI and TABPT at 303 K

Inhibitor	C (ppm)	R_p (Ω Cm^2)	C_{dl} (μF Cm^{-2})	IE_{EIS} (%)
BLANK	0	27.99	315.7	-
IABPI	200	181.5	73.87	84.57
	300	211.1	61.45	86.74
	400	237.4	49.31	88.20
	500	286.3	45.02	90.22
TABPT	200	294.0	57.37	90.47
	300	335.9	54.00	91.66
	400	455.4	50.42	93.85
	500	648.3	43.90	95.68

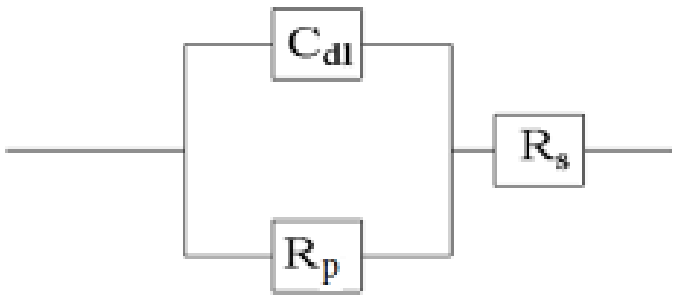

Fig. 10. Equivalent circuit for electrochemical impedance spectra

3.8 EDX Morphological Studies

EDX studies were performed to find out the existence of elements on the surface of MS in the absence and presence of inhibitors in 0.5 M H_2SO_4 and are shown in Fig. 11. Polished EDX spectrum of MS sample confirms the absence of oxide film and it was further confirmed by the absence of oxygen peak in Fig. 11a. But in the presence of IABPI and TABPT, EDX spectra were found to show the peaks for the presence of nitrogen, oxygen and sulphur indicating binding nature of inhibitors on the MS surface (Figs. 11b and 11c).

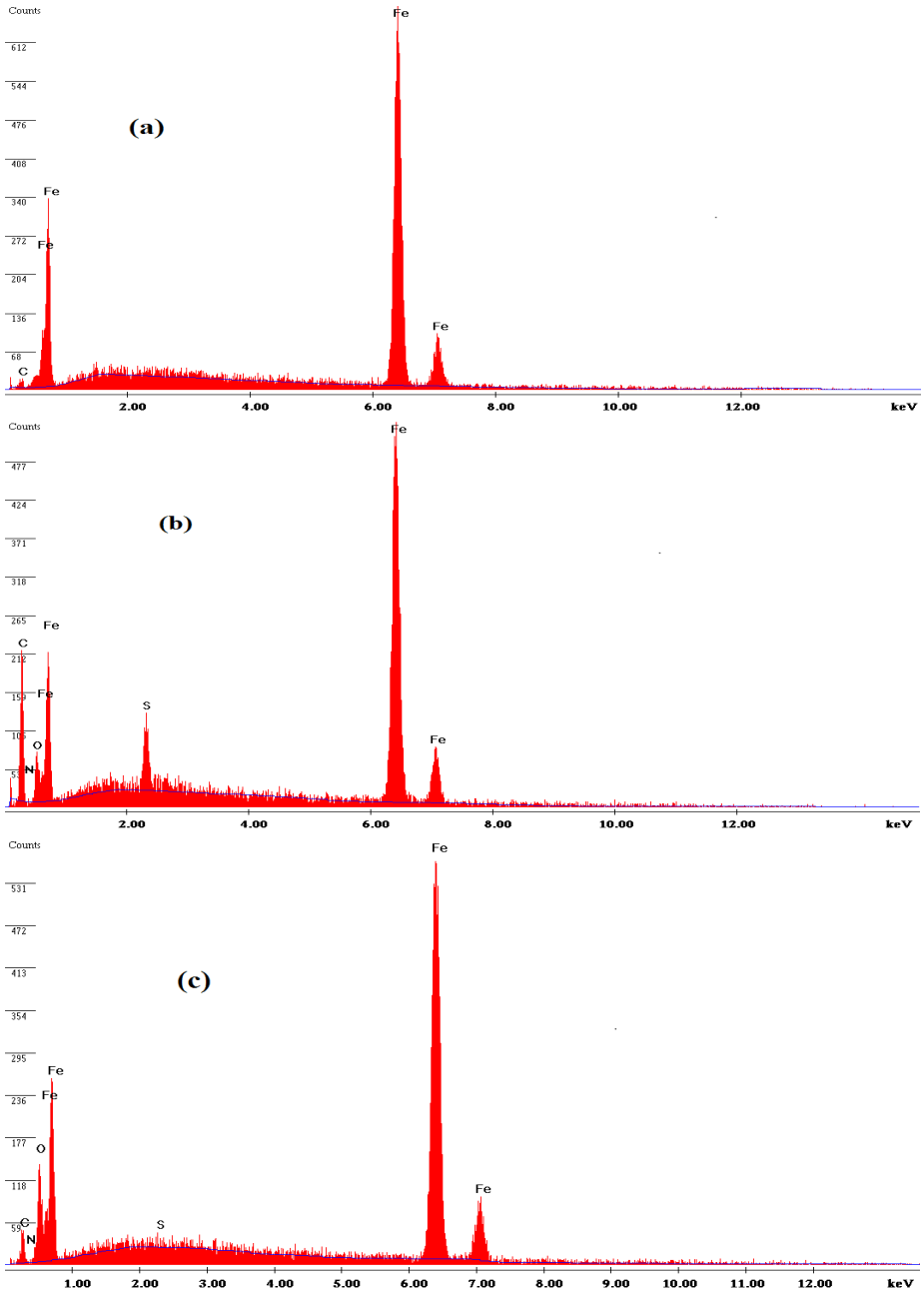

Fig. 11. EDX spectra of (a) polished MS (b) MS in presence of IABPI and (c) MS in presence of TABPT

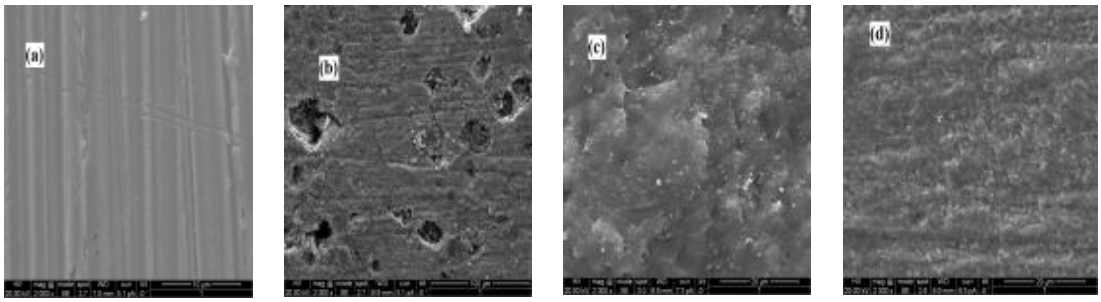

Fig. 12. SEM images of (a) MS polished surface (b) MS in 0.5 M H_2SO_4 (c) MS in the presence of IABPI and (d) MS in the presence of TABPT

3.9 SEM Studies

SEM images are used to understand the morphological interpretation of MS in the absence and presence of IABPI and TABPT. The SEM image of polished MS surface is shown in above Fig. 12a. The SEM image of MS surface in the absence of inhibitor in 0.5 M H_2SO_4 was found to be corroded seriously with the formation of many cracks and pits (Fig. 12b). Figs. 12c and 12d show the SEM morphology of MS surface in the presence of IABPI and TABPT, which clearly indicate the thin uniform coating of inhibitor molecules on the metal surface.

4. CONCLUSION

The inhibition efficiency of the synthesized dapsone derivatives in 0.5 M H_2SO_4 on MS corrosion was dependent on immersion time, temperature and inhibitor concentration. The percentage inhibition efficiencies obtained by mass loss, potentiodynamic polarization and electrochemical impendence spectroscopy (EIS) methods, were 82.31 - 95.68, 84.34 - 95.93 and 84.57 - 95.68%, respectively. Adsorption of inhibitors on MS surface obeyed Langmuir isotherm model. The values of Gibbs free energy of adsorption of the studied inhibitors were in the range of -36.81 to -39.45 kJ mol^{-1}, confirming both physisorption and chemisorption mechanism.

ACKNOWLEDGEMENTS

One of the authors (MPC) is grateful to University of Mysore for awarding SRF to carry out the research work.

COMPETING INTERESTS

Authors have declared that no competing interests exist.

REFERENCES

1. Nathan CC. Corrosion inhibitors. National association of corrosion engineering's, Houston, Texus; 1997.
2. Pradeep Kumar CB, Mohana KN, Muralidhara HB. Electrochemical and thermodynamic studies to evaluate the inhibition effect of synthesized piperidine derivatives on the corrosion of mild steel in acidic medium. Ionics. 2015;21:263-281.
3. Pradeep Kumar CB, Mohana KN. Corrosion inhibition efficiency and adsorption characteristics of some Schiff bases at mild steel/hydrochloric acid interface. J Taiwan Inst Chem. 2014;45: 1031–1042.
4. Chakravarthy MP, Mohana KN, Pradeep Kumar CB. Corrosion inhibition effect and adsorption behaviour of nicotinamide derivatives on mild steel in hydrochloric acid solution. Inter J Indus Chem; 2014. DOI: 10.1007/s40090-014-0019-3.
5. Chakravarthy MP, Mohana KN, Inhibition behaviour of some isonicotinic acid hydrazides on the corrosion of mild steel in hydrochloric acid solution. Inter J Corros; 2013. Article ID 854781. Available:http://dx.doi.org/10.1155/2013/854781
6. Moretti G, Guidi F, Grion G. Tryptamine as a green iron corrosion inhibitor in 0.5 M deaerated sulphuric acid. Corros Sci. 2006;46:387-403.
7. Abd El-Maksoud SA. The effect of organic compounds on the electrochemical behaviour of steel in acidic media - A review. Inter J Electrochem Sci. 2008;3: 528-555.
8. Quraishi MA, Sardar R. Corrosion inhibition of mild steel in acid solutions by some aromatic oxadiazoles. Mater. Chem Phys. 2003;78:425-431.

9. Sachin MS, Bilgic S, Yilmaz H. The inhibition effects of some cyclic nitrogen compounds on the corrosion of the steel in NaCl mediums. Appl Surf Sci. 2002;195:1-7.
10. Abdulla M, Al-Agez M, Fouda AS. Phenyl hydrazone derivatives as corrosion inhibitors for α-brass in hydrochloric acid solutions. Inter J Electrochem Sci. 2009;4: 336-352.
11. Bouklah M, Aouniti A, Hammouti B, Benkaddour M, Lagrenee M, Bentiss F. Effect of the substitution of an oxygen atom by sulphur in a pyridazinic molecule towards inhibition of corrosion of steel in 0.5 M H_2SO_4 medium. Prog Org Coat. 2004;51:118-124.
12. Bentiss F, Traisnel M, Vezin H, Hildebrand HF, Lagrenee M. 2,5-Bis(4-dimethylaminophenyl)-1,3,4-oxadiazole and 2,5-Bis(4-dimethylaminophenyl)-1,3,4-thiadiazole as corrosion inhibitors for mild steel in acidic media. Corros Sci. 2004;46: 2781-2792.
13. Wang H, Liu R, Xin. Inhibiting effects of some mercapto-triazole derivatives on the corrosion of mild steel in 1.0 M HCl medium. Corros Sci. 2004;46:2455-2466.
14. Karakus M, Sahin M, Bilgic S. An investigation on the inhibition effects of some new dithiophosphonic acid monoesters on the corrosion of the steel in 1 M HCl medium. Mater Chem Phys. 2005; 92:565-571.
15. Afidah A, Rahim E, Rocca J, Steinmetz MJ, Kassim RA, Sani Ibrahim M. Mangrove tannins and their flavanoid monomers as alternative steel corrosion inhibitors in acidic medium. Corros Sci. 2007;49:402-417.
16. Li W, He Q, Pei C, Hou B. Experimental and theoretical investigation of the adsorption behaviour of new triazole derivatives as inhibitors for mild steel corrosion in acid media. Electrochim Acta. 2007;52:6386-6394.
17. Sankarapapavinasam S, Pushpanaden F, Ahmed MF. Inhibition of mild steel corrosion in phosphoric acid solution by triazole derivatives. Corros Sci. 2006;48: 608-616.
18. Abdallah M, Al- Agez M, Fouda AS. Phenyl hydrazone derivatives as corrosion inhibitors for α-brass in hydrochloric acid solutions. Inter J Electrochem Sci. 2009;4: 336-352.
19. Ita BI, Abakedi OU, Osabor VN. Inhibition of mild steel corrosion in hydrochloric acid by 2-acetylpyridine and 2-acetylpyridine phosphate. Global Adv Res J Eng Tech. Innovation. 2013;2:084-089.
20. Wahyuningrum D, Achmad S, Syah YM, Buchari, Bundjali B, Ariwahjoedi B. The correlation between structure and corrosion inhibition activity of 4,5-diphenyl-1-vinylimidazole derivative compounds towards mild steel in 1% NaCl solution. Inter J Electrochem Sci. 2008;3:154-166.
21. Elewady GY. Pyridine derivatives as corrosion inhibitors for carbon steel in 2M hydrochloric acid solution. Inter J Electrochem Sci. 2008;3:1149-1161.
22. Venkatesan P, Anand B, Matheswaran P. Influence of formazan derivatives on corrosion inhibition of mild steel in hydrochloric acid medium. E J Chem. 2009;6:438-444.
23. Zarrouk A, Dafalil A, Hammouti B, Zarrok H, Boukhris S, Zertoubi M. Synthesis, characterization and comparative study of quinoxalines functionalized derivatives towards corrosion of mild steel in hydrochloric acid medium. Inter J Electrochem Sci. 2010;5:46-55.
24. Quraishi MA, Bhardwaj V, Rawat J. Prevention of metallic corrosion by lauric hydrazide and its salts under vapor phase conditions. J Am Oil Chem Soc. 2002;79: 603-609.
25. Jamesb AO, Oforkab NC, Abiola OK. Inhibition of acid corrosion of mild steel by pyridoxal and pyridoxol hydrochlorides. Inter J Electrochem Sci. 2007;2:278-284.
26. Bentiss F, Lagrenee M, Traisnel M, Mernari B, Elattari H. 3,5-bis(n-Hydroxyphenyl)-4-amino-1,2,4-triazoles and 3,5-bis(n-aminophenyl)-4-amino-1,2,4-triazoles: A new class of corrosion inhibitors for mild steel in 1M HCl medium. J Appl Electrochem. 1999;29:1073-1078.
27. Dubey RS, Potdar Y. Corrosion inhibition of 304 stainless steel in sodium chloride by ciprofloxacin and norfloxacin. Ind J Chem Tech. 2009;16:334-338.
28. Bentiss F, Lagrenee M, Traisnel M, Hornez JC. The corrosion inhibition of mild steel in acidic media by a new triazole derivative. Corros Sci. 1999;41:789-803.
29. Singh A, Singh AK, Quraishi MA. Dapsone: A novel corrosion inhibitor for mild steel in acid media. The Open Electrochem J. 2010;2:43-51.

30. Quraishi MA, Sharma HK. 4-Amino-3-butyl-5-mercapto-1,2,4-triazole: A new corrosion inhibitor for mild steel in sulphuric acid. Mater Chem Phys. 2002; 78:18-21.
31. Poornima T, Nayak J, Shetty AN. Corrosion inhibition of the annealed 18 Ni 250 grade maraging steel in 0.67 M Phosphoric acid by 3,4-dimethoxybenzaldehydethiosemicarbazone. Chem Sci J (CSJ). 2012;69:1-14.
32. Abdallah M, Heal EA, Fouda AS. Aminopyrimidine derivatives as inhibitors for corrosion of 1018 carbon steel in nitric acid solution. Corros Sci. 2006;48:1639-1654.
33. Abd El Rehim SS, Rafaey SAM, Taha F, Saleh MB, Ahmed RA. Corrosion inhibition of mild steel in acidic medium using 2-amino thiophenol and 2-cyanomethyl benzothiazole. J Appl Electrochem. 2001; 31:429-435.
34. Yurt A, Balaban A, Kandemir SU, Bereket G, Erk B. Investigation on some Schiff bases as HCl corrosion inhibitors for carbon steel. Mater Chem Phys. 2004;85: 420-426.
35. Tang L, Li X, Si Y, Mu G, Liu G. The synergistic inhibition between 8-hydroxyquinoline and chloride ion for the corrosion of cold rolled steel in 0.5 M sulfuric acid. Mater Chem Phys. 2006;95: 29-38.
36. Bhattacharya AK, Naiya TK, Mandal SN, Das SK. Adsorption, kinetics and equilibrium studies on removal of Cr(VI) from aqueous solutions using different low-cost adsorbents. Chem Eng J. 2008;137: 529-541.
37. Refaey SAM, Taha F, Abd El-Malak AM. Corrosion and inhibition of 316L stainless steel in neutral medium by 2-mercaptobenzimidazole. Inter J Electrochem Sci. 2006;1:80-91.
38. Li X, Deng S, Fu H. Three pyrazine derivatives as corrosion inhibitors for steel in 1.0 M H_2SO_4 solution. Corros Sci. 2011; 53:3241-3247.
39. Bouklah M, Hammouti B, Lagrenee M, Bentiss F. New thio-compounds as corrosion inhibitor for steel in 1 M HCl. Corros Sci. 2006;48:2470-2479.
40. Bayoumi FM, Ghanem WA. Corrosion inhibition of mild steel using naphthalene disulfonic acid. Mater Lett. 2005;59:3806-3809.
41. Yurt A, Balaban A, Ustun Kandemir S, Bereket G, Erk B. Investigation on some Schiff bases as HCl corrosion inhibitors for carbon steel. Mater Chem Phys. 2004;85: 420-426.
42. Li X, Deng S, Fu H, Li T. Adsorption and inhibition effect of 6-benzylaminopurine on cold rolled steel in 1.0 M HCl. Electrochim Acta. 2009;54:4089-4098.
43. Lebrini M, Bentiss F, Vezin H, Lagrenee M. Inhibiting effects of some oxadiazole derivatives on the corrosion of mild steel in perchloric acid solution. Appl Surf Sci. 2005;252:950-958.
44. Musa AY, Kadhum AAH, Mohamad AB, Takriff MS, Daud AR, Kamarudin SK. On the inhibition of mild steel corrosion by 4-amino-5-phenyl-4h-1, 2, 4-trizole-3-thiol. Corros Sci. 2010;52:526-533.
45. Juttner K. Electrochemical impedance spectroscopy (EIS) of corrosion processes on inhomogeneous surfaces. Electrochim Acta. 1990;35:1501-1508.
46. Bentiss F, Lebrini M, Langrenee M, Traisnel M, Elfarouk A, Vezin H. The influence of some new 2,5-disubstituted 1,3,4-thiadiazoles on the corrosion behaviour of mild steel in 1 M HCl solution: AC impedance study and theoretical approach. Electrochim Acta. 2007;52: 6865-6872.
47. El-Taib Heakal F, Ghoneim AA, Fekry AM. Stability of spontaneous passive films on high strength mo-containing stainless steels in aqueous solutions. J Appl Electrochem. 2007;37:405-413.
48. Lebrini M, Bentiss F, Vezin H, Lagrene M. The inhibition of mild steel corrosion in acidic solutions by 2,5-bis(4-pyridyl)-1,3,4-thiadiazole: Structure–activity correlation. Corros Sci. 2006;48:1279-1291.
49. Shukla SK, Quaraishi MA. The effects of pharmaceutically active compound doxycycline on the corrosion of mild steel in hydrochloric acid solution. Corros Sci. 2010;52:314-321.
50. Bentiss F, Traisnel M, Lagrenee M. The substituted 1,3,4-oxadiazoles: A new class of corrosion inhibitors of mild steel in acidic media. Corros Sci. 2000;42:127-146.
51. Parameswari K, Chaitra S, Nusrath Unnisa C, Selvaraj A. Effect of azlactones on corrosion inhibition of mild steel in acid medium. J Appl Sci Res. 2010;6:1100-1110.

52. Aloui S, Forsal I, Sfaira M, Ebn Touhami M, Taleb M, Filali Baba M, Daoudi M. New mechanism synthesis of 1,4-benzothiazine and its inhibition performance on mild steel in hydrochloric acid. Portugaliae Electrochim Acta. 2009;27:599-613.
53. Zaafarany I. Phenyl phtahlimide as corrosion inhibitor for corrosion of c-steel in sulphuric acid solution. Portugaliae Electrochim Act. 2009;27:631-643.
54. Ahamad I, Quraishi MA. Bis (benzimidazol-2-yl) disulphide: An efficient water soluble inhibitor for corrosion of mild steel in acid media. Corros Sci. 2009;51:2006-2013.

Peer-review history:
The peer review history for this paper can be accessed here:
http://www.sciencedomain.org/review-history.php?iid=1161&id=16&aid=9733